



This is a repository copy of *A highly anisotropic and hydrolytically degradable pickering emulsifier for oil-in-water emulsions.*

White Rose Research Online URL for this paper:

<https://eprints.whiterose.ac.uk/228525/>

Version: Accepted Version

Article:

Tyler, J.J.S., Farmer, M.A.H. orcid.org/0009-0008-9645-6921, Mykhaylyk, O.O. orcid.org/0000-0003-4110-8328 et al. (3 more authors) (2025) A highly anisotropic and hydrolytically degradable pickering emulsifier for oil-in-water emulsions. *Langmuir*. ISSN 0743-7463

<https://doi.org/10.1021/acs.langmuir.5c01134>

© 2025 The Authors. Except as otherwise noted, this author-accepted version of a journal article published in *Langmuir* is made available via the University of Sheffield Research Publications and Copyright Policy under the terms of the Creative Commons Attribution 4.0 International License (CC-BY 4.0), which permits unrestricted use, distribution and reproduction in any medium, provided the original work is properly cited. To view a copy of this licence, visit <http://creativecommons.org/licenses/by/4.0/>

Reuse

This article is distributed under the terms of the Creative Commons Attribution (CC BY) licence. This licence allows you to distribute, remix, tweak, and build upon the work, even commercially, as long as you credit the authors for the original work. More information and the full terms of the licence here:

<https://creativecommons.org/licenses/>

Takedown

If you consider content in White Rose Research Online to be in breach of UK law, please notify us by emailing eprints@whiterose.ac.uk including the URL of the record and the reason for the withdrawal request.



eprints@whiterose.ac.uk
<https://eprints.whiterose.ac.uk/>

A highly anisotropic and hydrolytically degradable Pickering emulsifier for oil-in-water emulsions

J. J. S. Tyler^a, M. A. H. Farmer^a, O. O. Mykhaylyk^a, M. J. Orchard^b, O. M. Musa^b
and S. P. Armes^{a,*}

*a. Dainton Building, Department of Chemistry, University of Sheffield, Brook Hill, Sheffield,
South Yorkshire, S3 7HF, UK.*

b. Ashland Specialty Ingredients, 1005 US 202/206, Bridgewater, New Jersey, 08807, USA.

* To whom correspondence should be addressed (s.p.arnes@sheffield.ac.uk)

Abstract. Highly anisotropic poly(*L*-lactide)-based block copolymer nanoparticles are prepared by the judicious combination of *reverse sequence* polymerization-induced self-assembly (PISA) with crystallization-driven self-assembly (CDSA). Such nanoparticles can be efficiently prepared as a 30% w/w aqueous dispersion and possess a distinctive diamond platelet morphology as judged by transmission electron microscopy. X-ray diffraction studies confirm the semicrystalline nature of the poly(*L*-lactide) block while atomic force microscopy analysis suggests a mean thickness of approximately 6 nm for the dried platelets. Small-angle X-ray scattering studies suggest that these platelets form localized tactoids at copolymer concentrations as low as 1.0% w/w. Herein we evaluate these platelets as a hydrolytically degradable Pickering emulsifier for the preparation of oil-in-water emulsions using various oils. In the case of squalane, systematic variation of the copolymer concentration and the high-shear homogenization conditions enabled the mean oil droplet diameter to be varied from approximately 40 μm to 125 μm . Fluorescein-labeled platelets were imaged on the surface of oil droplets using confocal microscopy. Such studies indicate submonolayer coverage even under optimized conditions, which may account for the unexpected long-term instability observed for such Pickering emulsions.

Introduction

Pickering emulsions are typically either oil or water droplets stabilized by particles.¹⁻³ Spontaneous adsorption of the particles at the oil-water interface reduces the interfacial area between the two immiscible fluids, which lowers the free energy of the system. A wide range of colloidal particles can act as a Pickering emulsifier: the key parameter is the surface wettability, often expressed as the particle contact angle.^{3,4} In general, using hydrophilic particles leads to the formation of oil-in-water emulsions, whereas employing hydrophobic particles usually produces water-in-oil emulsions.⁵ Compared to conventional surfactant-stabilized emulsions, Pickering emulsions typically offer higher long-term stability, greater reproducibility, and reduced foaming problems during high-shear homogenization.^{3,6}

In particular, various types of clay platelets have been evaluated as Pickering emulsifiers.⁷⁻¹⁶ For example, Ashby and Binks reported that stable toluene-in-water emulsions could be obtained in the presence of synthetic clay particles (Laponite RD), but only if such disk-like particles were first flocculated *via* added salt.¹² Similarly, Bon and co-workers used Laponite clay particles to stabilize emulsions of various vinyl monomers prior to their polymerisation.^{16,13} In this case, scanning electron microscopy and atomic force microscopy studies of the resulting so-called 'armored' latex particles suggested that the clay disks adsorbed flat at the latex surface. Mulqueen et al. utilized surface-aminated kaolin clay particles to stabilize micrometer-sized oil droplets, with *in situ* crosslinking leading to the formation of clay-based colloidosomes.¹⁷ Mayr and Breu reported that the combination of poly(ethylene imine) with a synthetic hectorite clay enabled the preparation of micrometer-sized oil-in-water emulsions using a multi-component hydrophobic fragrance comprising citronellol, eucalyptol, α -pinene, limonene and ethyl-2-methylbutyrate.¹⁴ Unlike prior reports,^{11,15} the synthetic cationic polymer was only introduced once the clay particles were either at or close to the oil-water interface to prevent their flocculation. This approach was essential to obtain microcapsules with optimum release profiles (maximum fragrance retention).

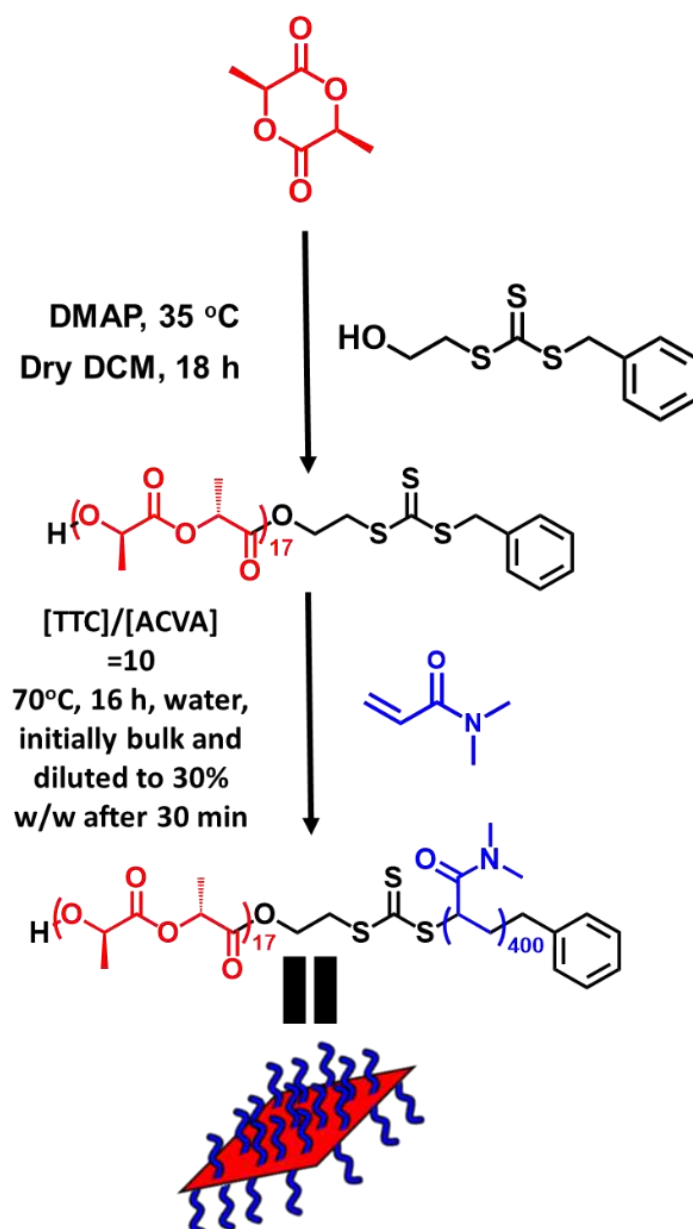
Polymerization-induced self-assembly (PISA) offers a versatile route to a wide range of sterically-stabilized block copolymer nanoparticles of controllable size and morphology.^{18–20} Depending on the target block composition, the final copolymer morphology can be spheres, worms or vesicles. Each of these nanoparticle morphologies has been examined in the context of Pickering emulsions.²¹ Worms are significantly more effective Pickering emulsifiers than the equivalent spheres,²² while framboidal vesicles adsorb much more strongly at the oil-water interface than smooth vesicles.²³ Pickering emulsifier efficiency is adversely affected by even relatively low levels of charge within the steric stabilizer chains,²⁴ while sufficiently small spherical nanoparticles can be used to prepare Pickering nanoemulsions via high pressure microfluidization processing of an initial coarse Pickering emulsion.

24–28

In 2018, Inam and co-workers reported the synthesis of poly(*L*-lactide)-poly(2-(dimethylamino)ethyl methacrylate) (PLLA-PDMAEMA) nanoparticles.²⁹ The semicrystalline nature of the PLLA block led to crystallization-induced self-assembly (CDSA), which produced a distinctive diamond platelet morphology. However, their synthetic route involved reversible addition-fragmentation chain transfer (RAFT) polymerization of DMAEMA in 1,4-dioxan at 70 °C, removal of the trithiocarbonate end-groups using excess azo initiator in DMF at 100 °C, post-polymerization processing via CDSA in hot ethanol for 4 h, and finally ageing a 0.5% w/w copolymer dispersion in ethanol at 20 °C for 24 h. Impressive control over the platelet size and morphology was certainly achieved, but this multi-step route is not readily scalable. Nevertheless, such micron-sized platelets were evaluated as Pickering emulsifiers for the preparation of water-in-water emulsions.²⁹

Herein we report the use of highly anisotropic diblock copolymer nanoparticles as a Pickering emulsifier for the preparation of oil-in-water emulsions. A recently reported reverse sequence aqueous PISA formulation³⁰ is used for the efficient preparation of a concentrated aqueous dispersion of poly(*L*-lactide)-poly(*N,N'*-dimethylacrylamide) (PLLA-PDMAC) nanoparticles (see **Scheme 1**). CDSA occurs during this synthesis, which leads to the formation of diamond platelets similar to those

reported by Inam and co-workers.²⁹ Importantly, such highly anisotropic nanoparticles are prepared directly in water at up to 30% w/w solids. Hence this is a potentially interesting and scalable route to new organic Pickering emulsifiers. Moreover, the PLLA block should ensure the long-term hydrolytic degradation of such diamond platelets to afford water-soluble PDMAC chains plus lactic acid oligomers. In the present study, we examine the performance of such diamond platelets as Pickering emulsifiers for the preparation of oil-in-water emulsions.



Scheme 1. Synthesis of a 30% w/w Aqueous Dispersion of PLLA₁₇-PDMAC₄₀₀ Diblock Copolymer Diamond Platelets by Combining Reverse Sequence Aqueous PISA with CDSA.

Experimental

Materials

All materials were used as received, unless stated otherwise. Squalane, *n*-dodecane, 4,4'-azobis(4-cyanovaleric acid) (ACVA; 98%), *N,N*-dimethylacrylamide (DMAC; 99%), castor oil, silicone oil, isopropyl myristate (98%) and fluorescein *o*-acrylate (FIA; 95%) were purchased from Sigma Aldrich (Dorset, UK). 4-(Dimethylamino)pyridine (DMAP) was purchased from Alfa Aesar (Heysham, UK). Methanol, isopropyl alcohol (IPA) and L-lactide (LLA: >98%) were purchased from Fisher Scientific (Loughborough, UK). The latter monomer was recrystallized from toluene before use. Dimethylformamide (DMF) was purchased from VWR (Leicestershire, UK). Deuterated dichloromethane (99.8%) was purchased from Goss Scientific Instruments Ltd (Cheshire, UK). Sunflower oil was purchased from a local supermarket. Benzyl 2-hydroxyethyl trithiocarbonate (BHETTC) was prepared using a literature protocol.³¹ Anhydrous DCM was obtained from an in-house Grubbs purification system. Deionized water (resistivity = 15 MΩ cm) was obtained from an Elgastat Option 3A water purification unit.

Anionic ring-opening polymerization of L-lactide using BHETTC initiator

This synthetic protocol has been previously reported by Farmer et al.³⁰ Briefly, LLA (5.25 g, 36.4 mmol), BHETTC (0.445 g, 1.82 mmol; target degree of polymerization, DP = 20) and DMAP (0.664 g) were added to a nitrogen-filled flame-dried Schlenk flask. Dry dichloromethane (28 mL) was added to the flask and the resulting reaction solution was stirred at 38°C for 23 h under a nitrogen atmosphere. The PLLA was precipitated by adding the reaction mixture to a ten-fold excess of ice-cold methanol (300 mL), isolated by vacuum filtration, washed once with ice-cold methanol and then twice with methanol at ambient temperature.

Synthesis of PLLA₁₇-PDMAC₄₀₀ diblock copolymer platelets

A typical synthesis of PLLA-PDMAC diblock copolymer platelets was conducted using the protocol reported by Farmer et al.³⁰ DMAC (1.47 g, 14.8 mmol), PLLA-TTC (0.100 g, 37.1 μmol; DMAC/PLLA molar ratio = 400), and ACVA (1.00 mg, 3.71 μmol; PLLA-TTC/ACVA molar ratio = 10) were added to a 14 mL glass vial charged with a magnetic flea, and degassed with nitrogen for 30 min. This reaction solution was then immersed in an oil bath set at 70°C and magnetically stirred until a significant increase in viscosity was observed. Degassed water (3.67 mL; preheated to 70°C) was then added to the vial using a degassed syringe and the resulting reaction mixture was briefly homogenized using a SciQuip Vortex VariMix (SciQuip Ltd, Rotherham, UK), before being stirred at 70 °C for 16 h.

Synthesis of PLLA₁₇-P(DMAC₄₀₀-stat-FLA_{0.1}) diblock copolymer platelets

The above synthesis protocol was employed, except that fluorescein-o-acrylate (1.40 mg, 3.71 μmol) was added to DMAC (1.47 g, 14.8 mmol) prior to the statistical copolymerization of these two comonomers.

Characterization of PLLA₁₇-PDMAC₄₀₀ diblock copolymer platelets

Gel permeation chromatography (GPC)

Molecular weight distributions were assessed using an Agilent 1260 Infinity GPC system equipped with a differential refractive index detector and a UV-visible variable wavelength detector. Two Agilent PL-gel 5 μm Mixed-C columns and a guard column were connected in series to this GPC system at an operating temperature of 60°C. The GPC eluent was DMF containing 10 mM LiBr and the flow rate was 1.0 mL min^{-1} . The refractive index detector was used to calculate molecular weights and dispersities by calibration against a series of eleven near-monodisperse poly(methyl methacrylate) standards with M_p values ranging from 2,380 g mol^{-1} to 2,200,000 g mol^{-1} . Samples were prepared for GPC analysis by dilution to 1.0% w/w using the DMF eluent, and chromatograms were analysed using Agilent GPC/SEC software.

Transmission electron microscopy

Transmission electron microscopy (TEM) studies were conducted using a FEI Tecnai Spirit 2 microscope equipped with an Orius SC1000B camera operating at 80 kV.

Formvar/Carbon-Copper grids (Electron Microscopy Sciences, UK) were treated with a plasma glow-discharge for 30 seconds to generate a hydrophilic surface. A 10 μL droplet of the freshly diluted 0.1% w/w aqueous copolymer dispersion was placed on a grid for 1 min, then blotted to remove excess sample. A 10 μL droplet of 0.75% w/v aqueous uranyl formate solution was then placed onto each grid using a micropipette, allowed to stand for 25 seconds, blotted to remove excess stain and then carefully dried with a vacuum hose. This protocol produced negatively stained grids.

¹H NMR spectroscopy

Spectra were recorded in CD_2Cl_2 using a 400 MHz Bruker Avance-400 spectrometer operating at 298 K, with 16 scans being averaged per spectrum. Aqueous copolymer dispersions were diluted with deuterated solvent and dried with anhydrous magnesium sulfate before passing through a 0.22 μm filter. The final monomer conversion was calculated by comparing integrated vinyl proton signals of the monomers ($\delta = 5.7, 6.3, 6.6$) to backbone signals of the precursor ($\delta = 5.2$).

X-Ray diffraction

Prior to X-ray diffraction (XRD) analysis, all aqueous dispersions were freeze-dried overnight. Powder XRD analysis was performed with Cu-K α radiation (40 kV, 40 mA) using a Bruker D8 ADVANCE X-ray powder diffractometer equipped with a motorized divergence slit for Bragg-Brentano geometry and a high-resolution energy-dispersive Lynxeye XE detector.

Preparation of Pickering emulsions

A typical preparation of a Pickering emulsion was conducted as follows. An aqueous dispersion of diblock copolymer platelets (2.40 mL, pH 6.6) was prepared at a known copolymer concentration and the desired model oil was added (0.60 mL, 20% v/v). High-shear homogenization was performed at 13,500 rpm for 2 min using an IKA UltraTurrax T-18 equipped with a 10 mm dispersing tool operating at 20 °C, unless otherwise stated.

Characterization of Pickering emulsions

Laser diffraction

A Malvern Mastersizer 3000 instrument equipped with a Hydro EV wet sample dispersion unit, a He-Ne laser ($\lambda = 633$ nm) and a LED blue light source ($\lambda = 470$ nm) was used for all laser diffraction measurements. The cell was cleaned using isopropyl alcohol (IPA) and the cell and dispersion unit were rinsed using a 70:30 IPA/water mixture, followed by a further three washes between each measurement using deionized water.

Optical microscopy

Optical microscopy images were recorded using a Cole–Palmer compound optical microscope equipped with a Moticam BTW digital camera.

Confocal microscopy

Confocal microscopy images were recorded using Zeiss LSM880 and LSM980 instruments (Zeiss, Jena, Germany), equipped with an Airyscan and an Airyscan 2 super-resolution detector respectively. The excitation wavelength was set to 495 nm and the emission maximum was collected at 520 nm. Images were analyzed using the Fiji distribution of *ImageJ* software.³²

Atomic Force microscopy

Atomic force microscopy (AFM) experiments were conducted using a Bruker Nanoscope VIII Multimode instrument, equipped with a J scanner, operating in tapping mode. A planar silicon wafer was washed with acetone and then cleaned via UV-ozone treatment for 30 min. A single droplet of a 0.1% w/w aqueous dispersion of PLLA₁₇-PDMAC₄₀₀ platelets was placed onto the silicon wafer using a

pipet and allowed to dry at ambient temperature. AFM images were analyzed using open source Gwyddion software.³³

Small-angle and wide-angle X-ray scattering

Small-angle and wide-angle X-ray scattering (SAXS and WAXS) patterns for 0.1-1.0% w/w copolymer concentration were recorded simultaneously at a synchrotron source (ESRF, station ID02, Grenoble, France) using monochromatic X-ray radiation ($\lambda = 0.1014$ nm) and an Eiger2 4M 2D detector (Dectris, Switzerland) for SAXS and an LX170-HS CCD 2D detector (Rayonix, USA) for WAXS. Dilute copolymer dispersions were injected in a custom-built flow-through cell comprising a glass capillary of 1.82 mm diameter. To avoid sample damage by the intense X-ray beam during data collection, the total exposure time of 1 s was subdivided into ten frames with an exposure time of 0.1 s per frame. Data were recorded at camera lengths of 2 m and 20 m, and the data were processed using standard beamline protocols. The resulting 2D SAXS and WAXS patterns were integrated to produce 1D patterns.^{34,35} These patterns were time-averaged and background-subtracted, and the SAXS data obtained at each camera length were merged using SAXSutilities2 software³⁶ to give an overall q range of 0.003 to 4.3 nm⁻¹, where $q = 4\pi \sin \theta / \lambda$ is the length of the scattering vector and θ is one-half of the scattering angle.

SAXS patterns were recorded for copolymer concentrations of 10-30% w/w using a laboratory-based SAXS beamline (Xeuss 2.0, Xenocs, Grenoble, France) equipped with a GeniX 3D Cu X-ray source, ($\lambda = 0.154$ nm), two sets of motorized scatterless slits for beam collimation and a Pilatus 1M 2D hybrid pixel detector (Dectris, Baden, Switzerland). Copolymer dispersions were injected into a custom-built flow-through cell, and SAXS patterns were recorded over a q range of 0.033 to 1.8 nm⁻¹. Data were reduced, calibrated, integrated and background-subtracted using Xenocs XSACT software supplied by the instrument manufacturer in combination with SAXSutilities2 software.³⁶

Dynamic Light Scattering

Dynamic light scattering (DLS) measurements were recorded using a Malvern NanoZS instrument at 25 °C. Scattered light was detected at 173° and hydrodynamic diameters were calculated using the Stokes–Einstein equation, which assumes dilute non-interacting spheres. Data were averaged over three consecutive measurements comprising ten runs per measurement.

Polarized Optical Microscopy

Polarized Optical Microscopy (POM) images were recorded using a Zeiss AxioScope A1 (Zeiss, Jena, Germany) equipped with crossed polarizers. Copolymer dispersions were loaded into glass sample

holders and transmitted light images were captured using an Axiocam 105 color camera; these images were subsequently processed using Zeiss Zen lite software.

Results and Discussion

Synthesis and characterization of diamond platelets

The PLLA₁₇ precursor was chain-extended with *N,N'*-dimethylacrylamide (DMAC) using a *reverse sequence* aqueous PISA formulation, as reported by Farmer et al. (see **Scheme 1**).³⁰ More specifically, the trithiocarbonate-functionalized PLLA₁₇ precursor (**Figure S1**) was dissolved in DMAC monomer and RAFT polymerization was initially conducted in the bulk at 70°C. The DMAC polymerization was allowed to proceed until a significant increase in viscosity was observed for the reaction mixture. Then degassed deionized water (preheated to 70°C) was added to dilute the reaction mixture at an intermediate DMAC conversion of 52% (which corresponds to an instantaneous PDMAC DP of 208), with brief vortex mixing to ensure a homogeneous reaction mixture. The DMAC polymerization was allowed to continue at 70°C for 16 h, targeting PLLA₁₇-PDMAC₄₀₀ platelets at 30% w/w solids. ¹H NMR spectroscopy studies indicated a final DMAC conversion of more than 99% (**Figure S2**). The corresponding fluorescently-labeled PLLA₁₇-P(DMAC₄₀₀-*stat*-FIA_{0.1}) platelets were prepared by statistical copolymerization of fluorescein acrylate with DMAC using essentially the same synthetic protocol. GPC analysis (**Figure 1a**) indicated that the RAFT polymerization was reasonably well-controlled ($M_w/M_n < 1.40$) in each case. XRD studies revealed the semicrystalline nature of both the PLLA₁₇-TTC precursor and the PLLA₁₇-PDMAC₄₀₀ diblock copolymer (**Figure 1b**): a Bragg peak was observed at a q value of 11.8 nm^{-1} (corresponding to a 2θ value of around 16.6°) in each diffraction pattern that corresponds with that reported in the literature.³⁷ For the PLLA₁₇-TTC precursor, the diffraction peaks at 10.6 nm^{-1} ($2\theta = 14.9^\circ$), 11.8 nm^{-1} (16.6°), 13.5 nm^{-1} (19.0°) and 15.8 nm^{-1} (22.4°) can be assigned to the 010, 110/200, 203/111 and 015 reflections of the α -phase of PLLA, respectively.³⁸ Inspecting the common diffraction peak at 11.8 nm^{-1} , the degree of crystallinity was calculated to be 51% for the PLLA₁₇ precursor and 5% for the PLLA₁₇-PDMAC₄₀₀ nanoparticles in powder form.

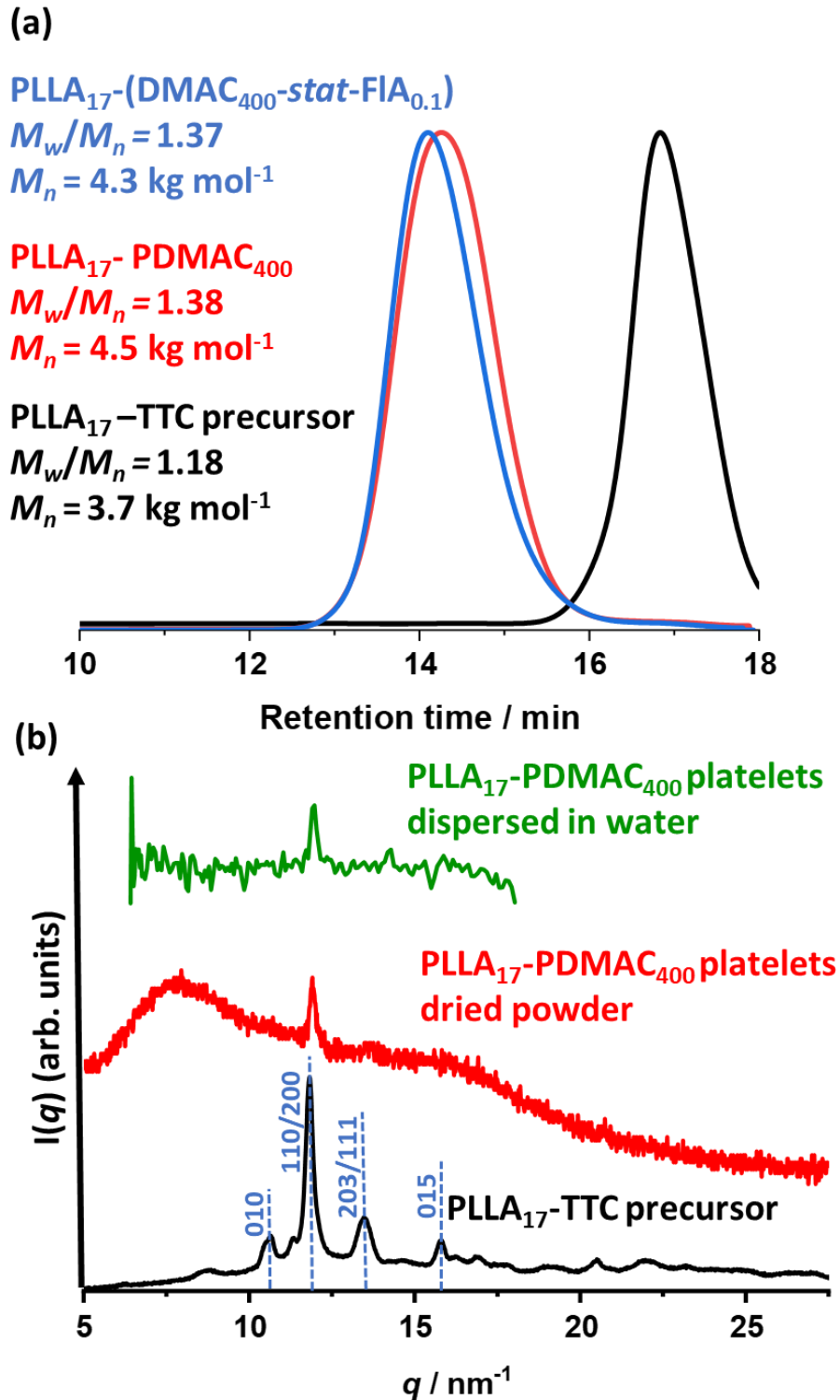


Figure 1. (a) GPC traces (refractive index detector) recorded for a $\text{PLLA}_{17}\text{-PDMAC}_{400}$ diblock copolymer, a $\text{PLLA}_{17}\text{-P(DMAC}_{400}\text{-stat-FIA}_{0.1})$ diblock copolymer and the corresponding $\text{PLLA}_{17}\text{-TTC}$ precursor; (b) XRD patterns recorded for $\text{PLLA}_{17}\text{-TTC}$ precursor (with peaks indexed) and freeze-dried $\text{PLLA}_{17}\text{-PDMAC}_{400}$ nanoparticles, plus a WAXS pattern recorded simultaneously with SAXS for a 1.0% w/w aqueous dispersion of $\text{PLLA}_{17}\text{-PDMAC}_{400}$ nanoparticles.

TEM analysis of the latter sample indicated a diamond platelet morphology (**Figure 2a-b**), which is consistent with that reported by Farmer et al.³⁰ A similar diamond platelet morphology was also observed for the PLLA₁₇-P(DMAC₄₀₀-*stat*-FIA_{0.1}) nanoparticles (**Figure 2c-d**).

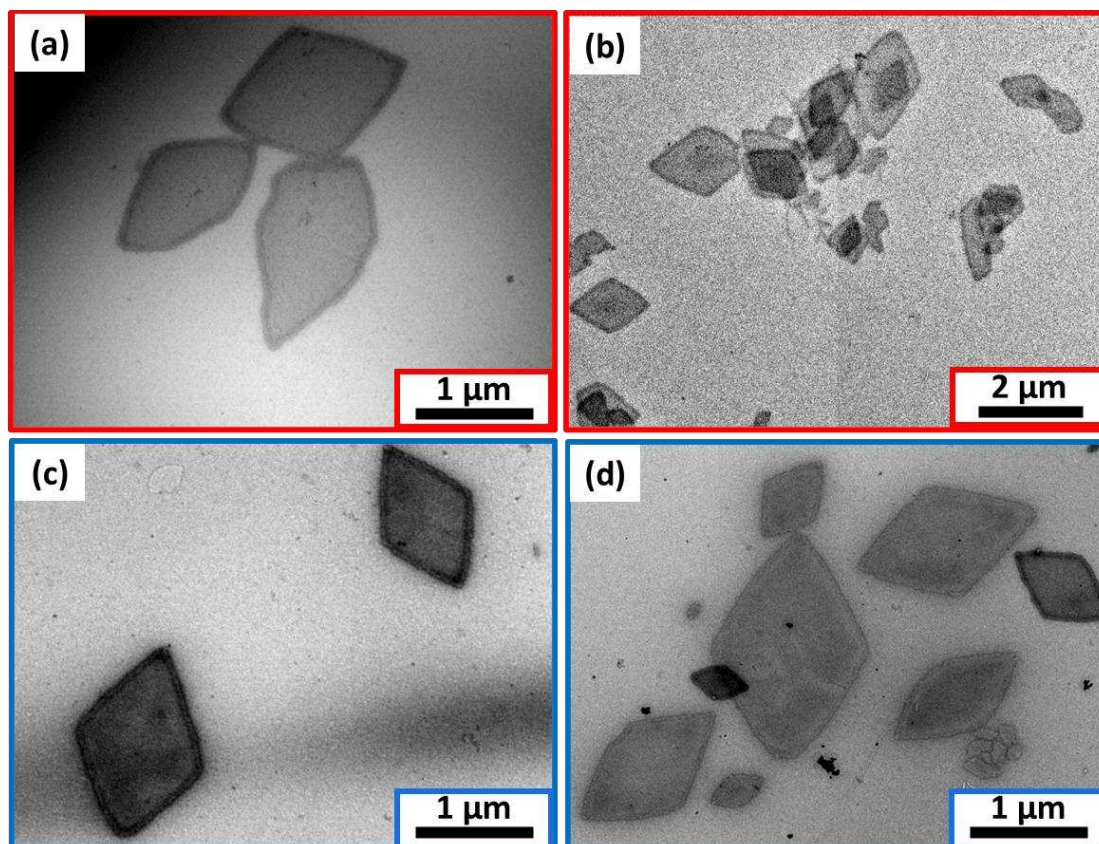


Figure 2. Representative TEM images recorded for (a, b) PLLA₁₇-PDMAC₄₀₀ platelets; (c, d) PLLA₁₇-P(DMAC₄₀₀-*stat*-FIA_{0.1}) platelets.

In principle, atomic force microscopy can be used to assess the mean thickness of these diamond platelets.²⁹ Accordingly, a dilute aqueous dispersion of PLLA₁₇-PDMAC₄₀₀ nanoparticles was allowed to dry on a silicon wafer to afford reasonably well-separated platelets at submonolayer coverage. An atomic force microscope operating in tapping mode was used to examine individual platelets (see **Figure 3**). Height profiles recorded across multiple platelets indicated a mean thickness of approximately 6 nm. This is significantly lower than the mean thickness of around 12 nm reported by Inam and co-workers for a series of PLLA₃₆-based diblock copolymer platelets²⁹ but is consistent with the shorter PLLA₁₇ block used in the present study. Clearly, these PLLA₁₇-PDMAC₄₀₀ diamond platelets can be regarded as highly anisotropic nanoparticles (mean aspect ratio = $500 \div 6 \approx 85$) that possess a relatively high specific surface area (see later).

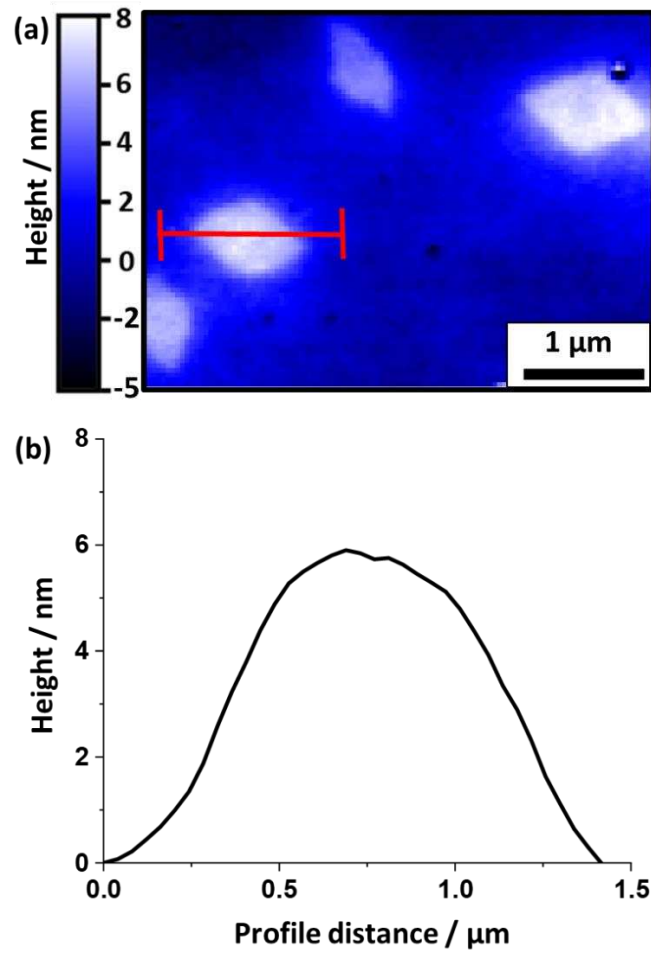


Figure 3. (a) AFM height image recorded for isolated PLLA₁₇-PDMAC₄₀₀ platelets deposited onto a planar silicon wafer and (b) representative height profile recorded across a single PLLA₁₇-PDMAC₄₀₀ platelet.

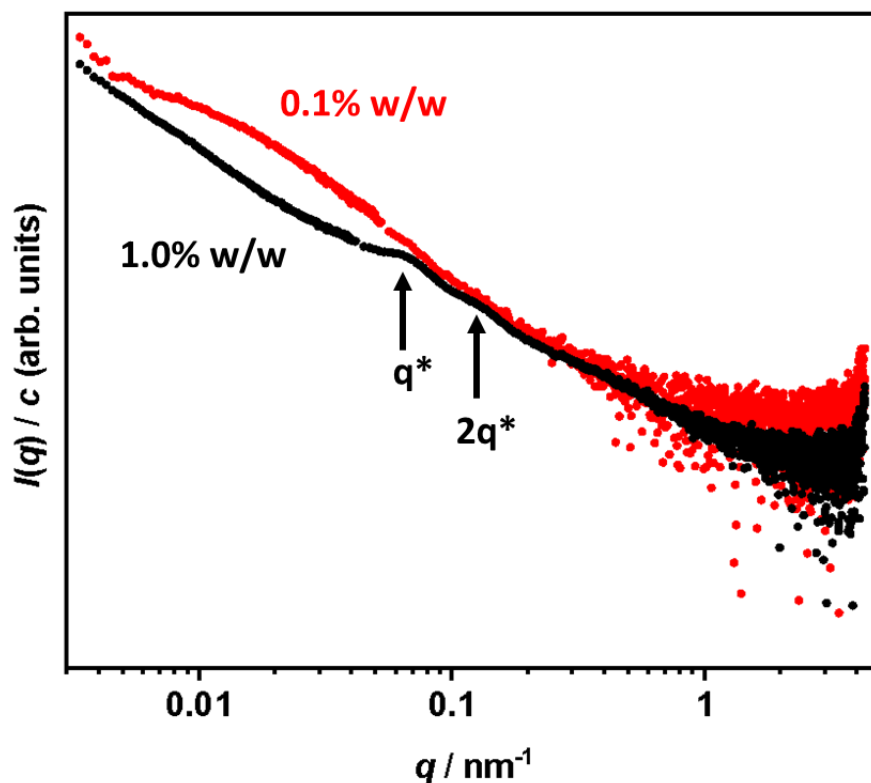


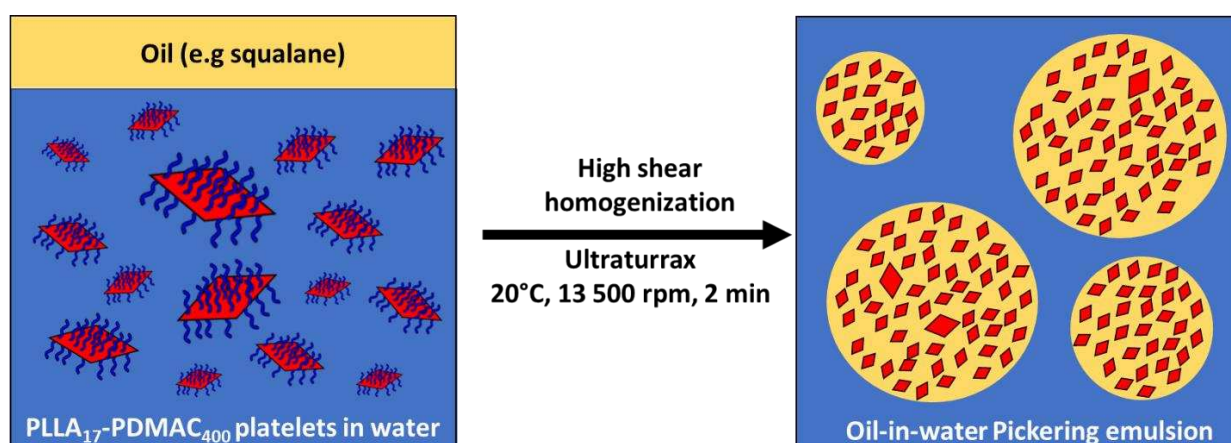
Figure 4. SAXS patterns recorded for PLLA₁₇-PDMAC₄₀₀ platelets at a copolymer concentration of either 0.1% (red data) or 1.0% w/w (black data). For both patterns, the SAXS intensity, $I(q)$, is normalized with respect to the copolymer concentration, c .

Small-angle X-ray scattering (SAXS) curves recorded for the PLLA₁₇-PDMAC₄₀₀ platelets at two copolymer concentrations are shown in **Figure 4**. At 1.0% w/w copolymer, two features are discernible at $q = 0.066$ and 0.130 nm^{-1} , which are denoted q^* and $2q^*$ respectively. Chi and co-workers recently reported a SAXS study³⁹ of similar-sized PLLA-based platelets dispersed in organic media at a copolymer concentration of 2.0% w/w and assigned such features to the first and second order diffraction peaks corresponding to a nematic phase. Alternatively, as suggested in a related SAXS study by the same authors,⁴⁰ they may indicate the presence of more localized tactoids comprising stacked diamond platelets. Indeed, both features disappear on dilution to 0.1% w/w, which is consistent with this interpretation. POM images recorded for aqueous dispersions of PLLA₁₇-PDMAC₄₀₀ platelets (**Figure S3**) reveal birefringence at or above a copolymer concentration of 1% w/w. Moreover, more intense birefringence is observed at higher copolymer concentrations, which suggests the presence of interparticle structure within such dispersions. Importantly, no Schlieren pattern was observed so there is no evidence for a nematic phase. In summary, the q^* and $2q^*$

features shown in **Figure 4** indicate the presence of localized tactoids comprising stacked diamond platelets with a mean period of approximately 96 nm.

To a good approximation, this latter scattering curve represents the form factor of the platelets. There are no discernible fringes in the high q region, which suggests a relatively high dispersity for the platelet cross-sectional thickness. However, fitting the Guinier equation [$I(q) \sim \exp(-q^2 R_g^2/3)$, where R_g is the radius of gyration of the scattering object] in the low q region indicates an R_g value of 170 nm for the platelets. Given their high aspect ratio (see above) and assuming that they can be approximated as flat disks, the known geometric relationship for disks [$R_g^2 = T^2/12 + R_d^2/2 \approx R_d^2/2$, where T is the disk thickness and R_d is the disk radius] indicates an R_d of around 240 nm.⁴¹ Thus, the mean platelet length (averaged over the long and short axes) – which is equal to the disk diameter – is calculated to approximately 480 nm. This value is reasonably consistent with the TEM and AFM images presented in **Figures 2** and **3**. Kratky plots (**Figure S4**) of integrated SAXS patterns recorded for aqueous dispersions of platelets at four copolymer concentrations reveal a local minimum, q^{**} , at approximately 0.84 nm^{-1} . This feature suggests a mean platelet thickness of 7.5 nm ,⁴⁰ which is in reasonably good agreement with the AFM data shown in **Figure 3**.

In addition, WAXS analysis of a 1.0% w/w copolymer concentration of diamond platelets indicates a characteristic peak at 11.8 nm^{-1} (**Figure 1b**), which corresponds to a d -spacing of around 5.32 \AA . This diffraction peak corresponds to the most intense 110 peak observed in the PLLA XRD pattern shown in **Figure 1b** and confirms that the PLLA chains retain their crystallinity within this colloidal dispersion of diamond platelets.



Scheme 2. Schematic cartoon to illustrate the preparation of oil-in-water Pickering emulsions using the PLLA₁₇-PDMAC₄₀₀ platelets described in this study.

Diamond platelet-stabilized Pickering emulsions

A series of oil-in-water Pickering emulsions were obtained (**Scheme 2**) when using various model oils at a relatively low PLLA₁₇-PDMAC₄₀₀ concentration of 0.025% w/w (**Figure 5**).

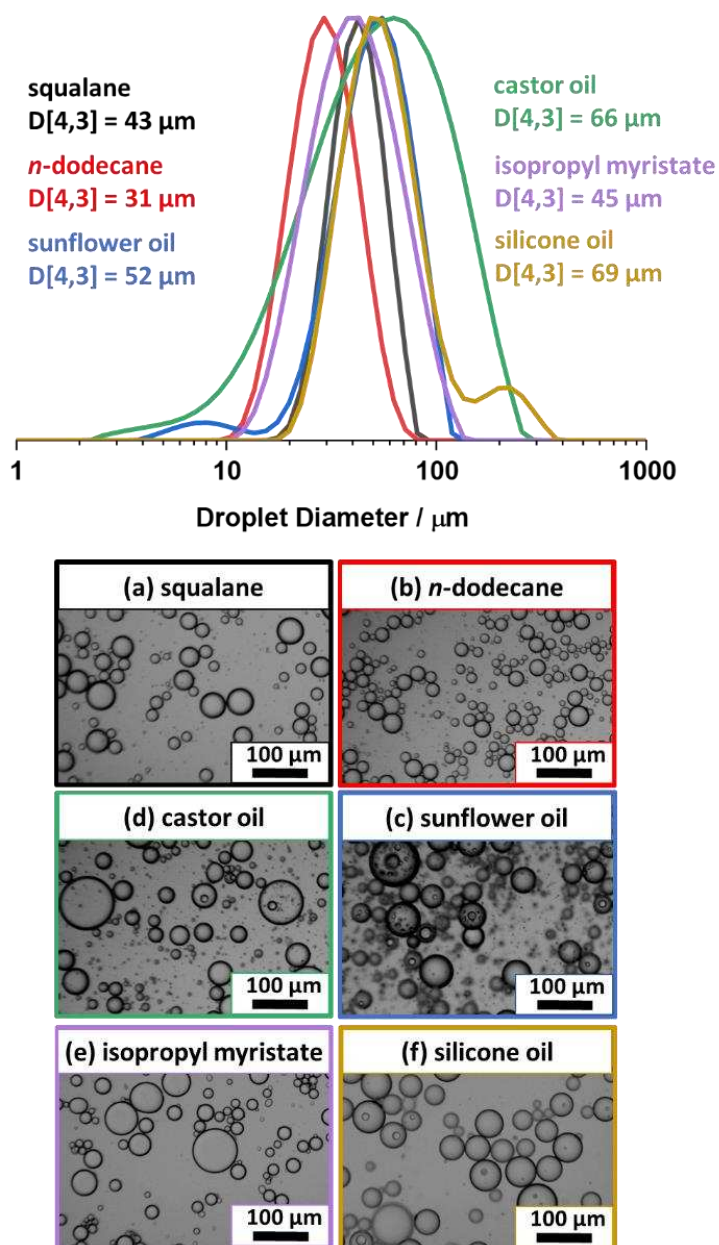


Figure 5. Laser diffraction droplet size distributions and representative optical micrographs recorded for oil-in-water Pickering emulsions prepared using the following model oils: (a) squalane, (b) *n*-dodecane, (c) sunflower oil, (d) castor oil, (e) isopropyl myristate and (f) silicone oil. Each emulsion was prepared via high-shear homogenization 13 500 rpm for 2 min using a 0.025 % w/w aqueous dispersion of PLLA₁₇-PDMAC₄₀₀ platelets and 20% v/v oil.

Emulsions based on squalane and *n*-dodecane (**Figure 5a-b**) exhibited narrower droplet size distributions and typically smaller droplets than those obtained using sunflower oil, castor oil, isopropyl myristate and silicone oil (**Figure 5c-f**). The remarkable efficacy of these highly anisotropic platelet particles as Pickering emulsifiers, even when utilized at relatively low concentration, can be attributed to their relatively high specific surface area (see later). Furthermore, the effective %area occupied by an individual platelet adsorbed at the oil-water interface is typically higher than that of spherical particles. This is because the entire face of a platelet can be in contact with the interface. For a spherical nanoparticle, this degree of interaction can only be achieved at a particle contact angle of 90°, corresponding to equal wetting of the particle by oil and water.^{3,42}

The PLLA₁₇-PDMAC₄₀₀ concentration was systematically varied to produce a series of squalane-in-water emulsions and the volume-average droplet diameter $D[4,3]$ was determined from laser diffraction analysis. Relatively stable oil droplets of around 125 μm diameter were obtained at a PLLA₁₇-PDMAC₄₀₀ concentration as low as 0.001% w/w. Increasing the copolymer concentration up to 0.025% w/w led to a three-fold reduction in the droplet diameter but no further reduction in size was observed thereafter (**Figure 6a** and **Table S1**). This suggests that this particular copolymer concentration lies close to the critical concentration at which almost all of the platelets become adsorbed at the surface of the oil droplets during high-shear homogenization. Variation of stirring rate also revealed a plateau in droplet size for stirring rates above 13 500 rpm up to 25 000 rpm. Comparison of TEM images recorded after high-shear homogenization at either 13 500 or 25 000 rpm, plus DLS data recorded for PLLA₁₇-PDMAC₄₀₀ dispersions before and after being subjected to high-shear homogenization at 25 000 rpm, revealed that the original diamond platelet morphology is partially degraded when the nanoparticles are subjected to the higher stirring rate (**Figure S5**). These observations account for the corresponding reduction in mean droplet diameter (**Figure 6b**, **Table S2**).

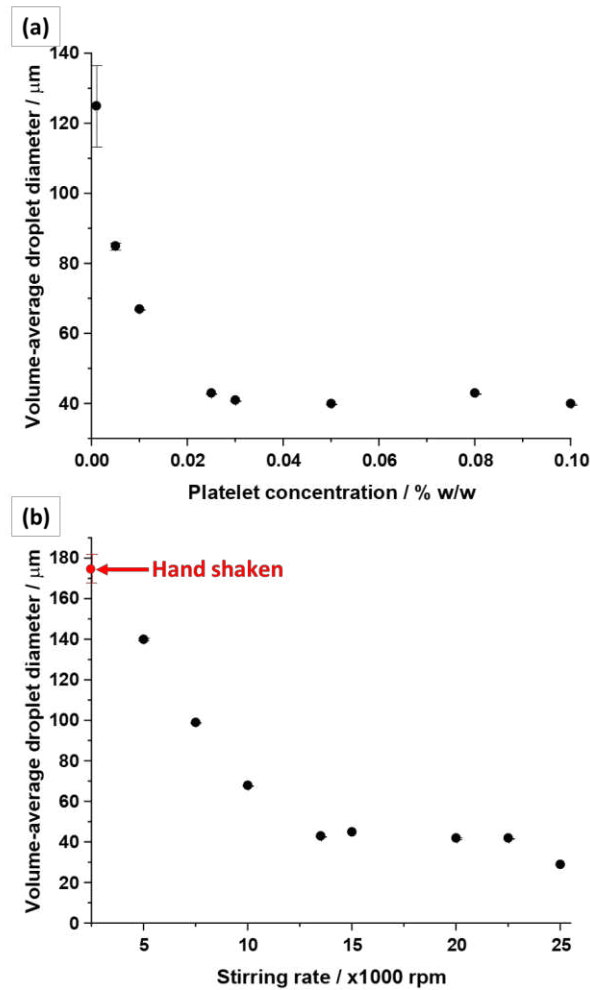


Figure 6. (a) Variation of volume-average droplet diameter, $D[4,3]$, with PLLA₁₇-PDMAC₄₀₀ platelet concentration for squalane-in-water Pickering emulsions prepared via high-shear homogenization at 13 500 rpm at 20 °C using 20% v/v squalane. (b) Variation of volume-average droplet diameter, $D[4,3]$, with stirring rate for squalane-in-water Pickering emulsions prepared using a 0.025% w/w aqueous dispersion of PLLA₁₇-PDMAC₄₀₀ platelets. Error bars are calculated based on the average of triplicate measurements, but they lie within the data points in almost all cases.

Laser diffraction data reveal that for squalane-in-water emulsions formed at platelet concentrations below 0.025 % w/w, a unimodal droplet size distribution is present, and decreases in size as platelet concentration is increased up to this point (**Figure 7a**). For concentrations above 0.025% a second, smaller population is observed at 1- 10 μm which increases in relative size as platelet concentration is further increased. This onset of a second smaller population with increasing concentration is also observed by optical microscopy (**Figure 7b-e**). This feature is tentatively attributed to the formation of aggregates comprising excess non-adsorbed platelets (**Figure S6**).

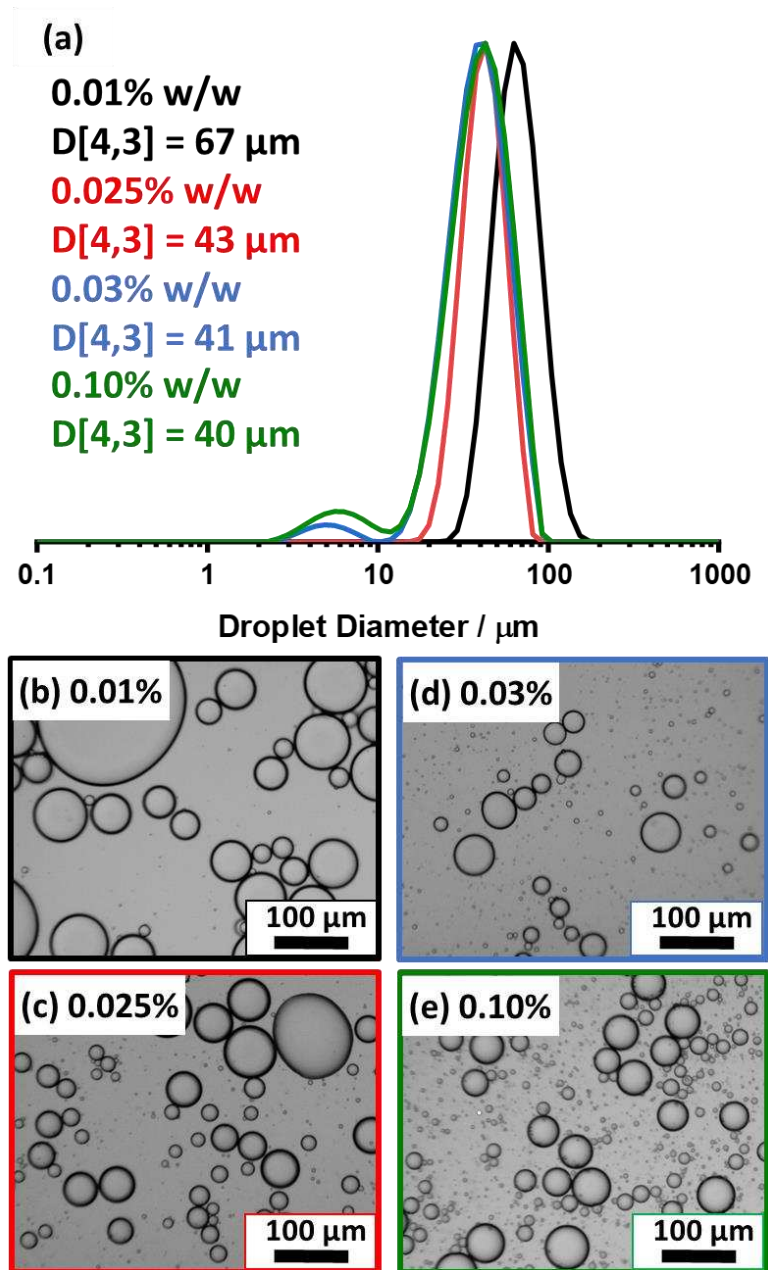


Figure 7. Laser diffraction droplet size distributions and representative optical micrographs obtained for a squalane-in-water Pickering emulsion prepared via high-shear homogenization of 20% v/v squalane at 13 500 rpm for 2 min at 20 °C using the following concentrations of PLLA₁₇-PDMAC₄₀₀ platelets: (a) 0.01% w/w, (b) 0.025% w/w, (c) 0.03% w/w, (d) 0.10% w/w.

A squalane-in-water Pickering emulsion was prepared on a larger scale (12 mL) using 20% v/v oil at a copolymer concentration of 0.025% w/w to enable the mean droplet diameter to be monitored by optical microscopy and laser diffraction over time at 20 °C (**Figure 8**). The initial droplet diameter of 53 μm was somewhat larger than that observed for the same emulsion prepared on a 3 mL scale (43 μm). The volume-average droplet diameter reported by laser diffraction did not change significantly within the first 72 h. However, a slightly broader distribution was obtained and optical micrographs suggest the presence of rather polydisperse droplets (**Figure 8a-c**). A distinctly bimodal droplet

distribution was obtained after ageing at 20 °C for one week, with a minor population at around 200-300 μm diameter. This suggests significant droplet growth and a population of larger droplets were observed by optical microscopy (**Figure 8d**). This minor population of coarse droplets became more prominent after ageing for three weeks and the corresponding optical micrographs revealed the presence of larger droplets (**Figure 8e**).

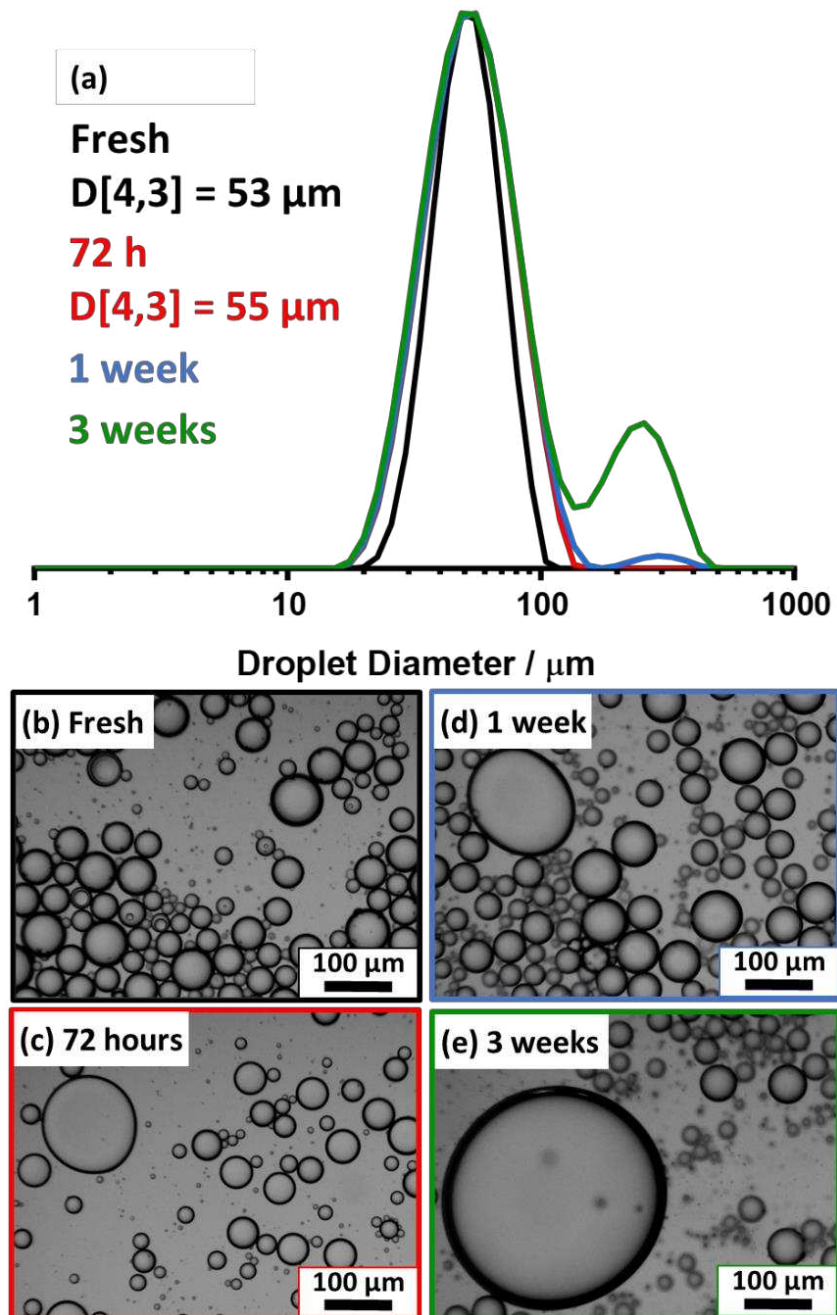


Figure 8. (a) Laser diffraction droplet size distributions obtained for a squalane-in-water Pickering emulsion prepared using 20% v/v squalane and 0.025% w/w PLLA₁₇-PDMAC₄₀₀ platelets via high-shear homogenization at 13 500 rpm for 2 min at 20 °C: fresh emulsion, after 72 h at 20 °C, after 1 week at 20 °C, and after 3 weeks at 20 °C. (b-e) Corresponding representative optical micrographs recorded for the same aging emulsion.

Confocal microscopy images recorded for squalane-in-water emulsions stabilized by fluorescently-labeled PLLA₁₇-PDMAC₄₀₀ platelets confirm the presence of platelets adsorbed at the surface of the oil droplets (**Figure 9**). The mean surface coverage of the droplets was estimated to be 27% by digital image analysis using *ImageJ* software.⁴³

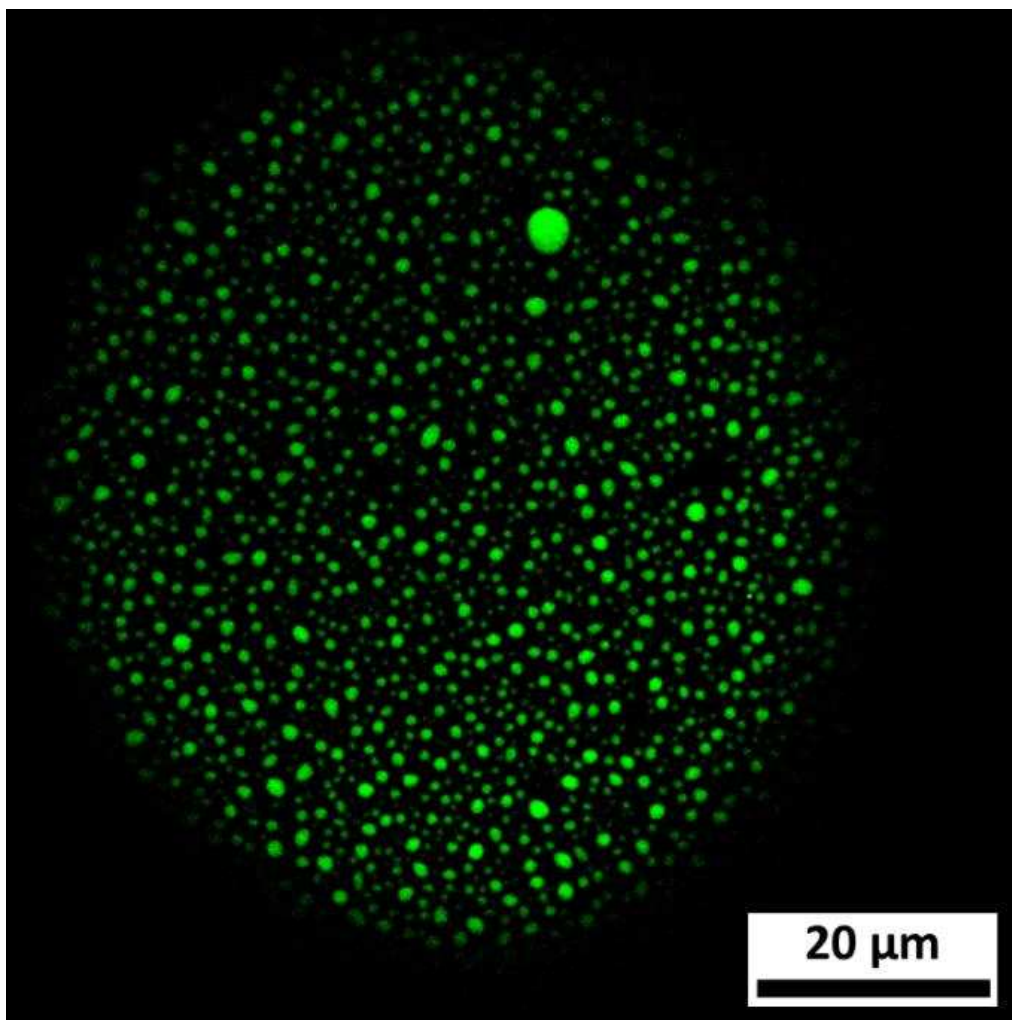


Figure 9. Confocal microscopy image recorded for fluorescein-labeled PLLA₁₇-PDMAC₄₀₀ platelets absorbed at the surface of a single squalane droplet. This squalane-in-water emulsion was prepared using 20% v/v squalane and a 0.025% w/w aqueous dispersion of PLLA₁₇-P(DMAC₄₀₀-*stat*-FIA_{0.1}) platelets via high-shear homogenization at 13 500 rpm for 2 min at 20 °C.

In a prior study, we reported that diblock copolymer worms of a given cross-sectional diameter are more effective Pickering emulsifiers than spheres of the same diameter.²² This is because highly anisotropic worms are more than one order of magnitude more massive than the spheres. Thus they adsorb much more strongly at the oil-water interface – yet exhibit a comparable (i.e., only around 33 % lower) specific surface area relative to the corresponding spheres. It is worth considering the diamond platelets in this context. To a good first approximation, their specific surface area, A_s , is given

by $A_s = 2/\rho \cdot t$, where ρ is the platelet density and t is the mean platelet thickness. Notably, A_s is independent of the platelet length. Assuming $\rho = 1.0 \text{ g cm}^{-3}$ and $t = 6 \text{ nm}$ (**Figure 3**), we calculate A_s to be approximately $330 \text{ m}^2 \text{ g}^{-1}$, which is relatively high. Compared to spheres with the same A_s value, the platelets are much more massive and their conformal contact area is relatively high when adsorbed at the oil-water interface. Thus it is not surprising that these diamond platelets can be used to prepare Pickering emulsions at relatively low copolymer concentrations (see **Figure 6a**). On the other hand, such emulsions exhibit relatively poor long-term stability compared to Pickering emulsions prepared using clay platelets.¹² This appears to be related to the relatively low surface coverage achieved for these diamond platelets at the oil-water interface (see **Figure 9**). In principle, this may be because the highly hydrophilic PDMAC steric stabilizer chains produce a relatively low particle contact angle, which would significantly reduce the interfacial adhesion energy.³ However, this tentative explanation would require further experiments for corroboration, which are beyond the scope of the current study.

Conclusions

In summary, PLLA₁₇-PDMAC₄₀₀ diblock copolymer nanoparticles have been prepared as a 30% w/w aqueous dispersion by combining *reverse sequence* polymerization-induced self-assembly (PISA) with crystallization-driven self-assembly (CDSA). TEM analysis confirms a distinctive diamond platelet morphology while SAXS studies indicate that these platelets form a nematic phase at a copolymer concentration as low as 1.0% w/w. XRD analysis confirm the semicrystalline nature of the poly(L-lactide) block, while atomic force microscopy analysis suggests a mean thickness of approximately 6 nm for the dried platelets. A series of oil-in-water Pickering emulsions has been prepared using PLLA₁₇-PDMAC₄₀₀ diamond platelets at a copolymer concentration as low as 0.025% w/w. This is attributed to the relatively specific surface area for such highly anisotropic nanoparticles. In the case of squalane, systematic variation of the copolymer concentration and the high-shear homogenization conditions enabled the mean oil droplet diameter to be varied from approximately 40 μm to 125 μm . The presence of fluorescently-labelled diamond platelets adsorbed at the surface of squalane droplets was confirmed by confocal microscopy studies. A relatively low surface coverage of 27% was estimated by digital image analysis, which is consistent with the poor long-term stability of such Pickering emulsions observed on standing at 20 °C. In principle, the semicrystalline PLLA chains that form the core of such diamond platelets should undergo hydrolytic degradation.³⁰

Acknowledgements

Ashland Specialty Ingredients (Bridgewater, New Jersey, USA) is thanked for financial support of this study and for permission to publish this work. We thank Darren Robinson and Nick Van Hateren at the Wolfson Light Microscopy Facility, School of Biological Sciences, University of Sheffield for their technical assistance with the confocal microscopy studies and acknowledge MRC grant MR/X012077/1 for access to the Zeiss LSM980 Airyscan 2 Confocal instrument. Aysha Mehter is thanked for assistance with the AFM experiments. The authors also thank the European Synchrotron Radiation Facility for providing beam time at the ID02 beamline (SC-5604).

Supporting Information Available

¹H NMR spectra recorded for the PLLA₁₇ precursor and the PLLA₁₇-PDMAC₄₀₀ diblock copolymer chains, polarized optical microscopy images recorded for PLLA₁₇-PDMAC₄₀₀ platelets at various copolymer concentrations, four Kratky plots of integrated SAXS patterns recorded for PLLA₁₇-PDMAC₄₀₀ platelets at various copolymer concentrations, tabulated additional laser diffraction data, additional TEM images, and further laser diffraction particle size distributions. The Supporting Information is available free of charge on the ACS Publications website.

References

- (1) Pickering, S. U. Emulsions. *J. Chem. Soc., Trans.* **1907**, *91*, 2001–2021.
- (2) Ramsden, W. Separation of Solids in the Surface-Layers of Solutions and ‘Suspensions’ (Observations on Surface-Membranes, Bubbles, Emulsions, and Mechanical Coagulation).—Preliminary Account. *Proc. R. Soc. London* **1904**, *72*, 156–164.
- (3) Binks, B. P. Particles as Surfactants - Similarities and Differences. *Curr. Opin. Colloid Interface Sci.* **2002**, *7*, 21–41.
- (4) Binks, B. P. Colloidal Particles at a Range of Fluid-Fluid Interfaces. *Langmuir* **2017**, *33*, 6947–6963.
- (5) Binks, B. P.; Isa, L.; Tyowua, A. T. Direct Measurement of Contact Angles of Silica Particles in Relation to Double Inversion of Pickering Emulsions. *Langmuir* **2013**, *29*, 4923–4927.
- (6) French, D. J.; Brown, A. T.; Schofield, A. B.; Fowler, J.; Taylor, P.; Clegg, P. S. The Secret Life of Pickering Emulsions: Particle Exchange Revealed Using Two Colours of Particle. *Sci. Rep.* **2016**, *6*, 1–9.
- (7) Kang, Y.; Zan, Y.; Cong, Y.; Wang, X.; Luo, Y.; Li, L. A Clay-Based Pickering Nanoemulsion with Antibacterial Activity. *Colloids Surfaces A Physicochem. Eng. Asp.* **2024**, *686*, 133337.
- (8) Garcia, P. C.; Whitby, C. P. Laponite-Stabilised Oil-in-Water Emulsions: Viscoelasticity and Thixotropy. *Soft Matter* **2012**, *8*, 1609–1615.
- (9) Yang, F.; Liu, S.; Xu, J.; Lan, Q.; Wei, F.; Sun, D. Pickering Emulsions Stabilized Solely by Layered Double Hydroxides Particles: The Effect of Salt on Emulsion Formation and Stability. *J. Colloid Interface Sci.* **2006**, *302*, 159–169.

- (10) Binks, B. P.; Clint, J. H.; Whitby, C. P. Rheological Behavior of Water-in-Oil Emulsions Stabilized by Hydrophobic Bentonite Particles. *Langmuir* **2005**, *21*, 5307–5316.
- (11) Cui, Y.; Van Duijneveldt, J. S. Microcapsules Composed of Cross-Linked Organoclay. *Langmuir* **2012**, *28*, 1753–1757.
- (12) Ashby, N. P.; Binks, B. P. Pickering Emulsions Stabilised by Laponite Clay Particles. *Phys. Chem. Chem. Phys.* **2000**, *2*, 5640–5646.
- (13) Teixeira, R. F. A.; McKenzie, H. S.; Boyd, A. A.; Bon, S. A. F. Pickering Emulsion Polymerization Using Laponite Clay as Stabilizer to Prepare Armored “Soft” Polymer Latexes. *Macromolecules* **2011**, *44*, 7415–7422.
- (14) Mayr, L.; Breyer, J. Encapsulation of Fragrance in Aqueous Emulsions by Delaminated Synthetic Hectorite. *Langmuir* **2020**, *36*, 11061–11067.
- (15) Williams, M.; Armes, S. P.; York, D. W. Clay-Based Colloidosomes. *Langmuir* **2012**, *28*, 1142–1148.
- (16) Bon, S. A. F.; Colver, P. J. Pickering Miniemulsion Polymerization Using Laponite Clay as a Stabilizer. *Langmuir* **2007**, *23*, 8316–8322.
- (17) Mulqueen, P. J.; Taylor, P.; Gittins, D. I. Microencapsulation Process for Producing Microcapsules Comprising a Surface-Modified Particulate Inorganic Material in a Cross-Linked Microcapsule Wall. WO/2009/063257, 2009.
- (18) D’Agosto, F.; Rieger, J.; Lansalot, M. RAFT-Mediated Polymerization-Induced Self-Assembly. *Angew. Chemie - Int. Ed.* **2020**, *59*, 8368–8392.
- (19) Canning, S. L.; Smith, G. N.; Armes, S. P. A Critical Appraisal of RAFT-Mediated Polymerization-Induced Self-Assembly. *Macromolecules* **2016**, *49*, 1985–2001.
- (20) Ikkene, D.; Six, J. L.; Ferji, K. Progress in Aqueous Dispersion RAFT PISA. *Eur. Polym. J.* **2023**, *118*, 111848.
- (21) Hunter, S. J.; Armes, S. P. Pickering Emulsifiers Based on Block Copolymer Nanoparticles Prepared by Polymerization-Induced Self-Assembly. *Langmuir* **2020**, *36*, 15463–15484.
- (22) Thompson, K. L.; Fielding, L. A.; Mykhaylyk, O. O.; Lane, J. A.; Derry, M. J.; Armes, S. P. Vermicious Thermo-Responsive Pickering Emulsifiers. *Chem. Sci.* **2015**, *6*, 4207–4214.
- (23) Mable, C. J.; Warren, N. J.; Thompson, K. L.; Mykhaylyk, O. O.; Armes, S. P. Framboidal ABC Triblock Copolymer Vesicles: A New Class of Efficient Pickering Emulsifier. *Chem. Sci.* **2015**, *6*, 6179–6188.
- (24) Hunter, S. J.; Penfold, N. J. W.; Chan, D. H.; Mykhaylyk, O. O.; Armes, S. P. How Do Charged End-Groups on the Steric Stabilizer Block Influence the Formation and Long-Term Stability of Pickering Nanoemulsions Prepared Using Sterically Stabilized Diblock Copolymer Nanoparticles? *Langmuir* **2020**, *36*, 769–780.
- (25) Thompson, K. L.; Cinotti, N.; Jones, E. R.; Mable, C. J.; Fowler, P. W.; Armes, S. P. Bespoke Diblock Copolymer Nanoparticles Enable the Production of Relatively Stable Oil-in-Water Pickering Nanoemulsions. *Langmuir* **2017**, *33*, 12616–12623.
- (26) Thompson, K. L.; Derry, M. J.; Hatton, F. L.; Armes, S. P. Long-Term Stability of n-Alkane-in-Water Pickering Nanoemulsions: Effect of Aqueous Solubility of Droplet Phase on Ostwald Ripening. *Langmuir* **2018**, *34*, 9289–9297.

- (27) Hunter, S. J.; Armes, S. P. Long-Term Stability of Pickering Nanoemulsions Prepared Using Diblock Copolymer Nanoparticles: Effect of Nanoparticle Core Crosslinking, Oil Type, and the Role Played by Excess Copolymers. *Langmuir* **2022**, *38*, 8021–8029.
- (28) Hunter, S. J.; Armes, S. P. Sterically Stabilized Diblock Copolymer Nanoparticles Enable Efficient Preparation of Non-Aqueous Pickering Nanoemulsions. *Langmuir* **2023**, *39*, 7361–7370.
- (29) Inam, M.; Jones, J. R.; Pérez-Madrigal, M. M.; Arno, M. C.; Dove, A. P.; O'Reilly, R. K. Controlling the Size of Two-Dimensional Polymer Platelets for Water-in-Water Emulsifiers. *ACS Cent. Sci.* **2018**, *4*, 63–70.
- (30) Farmer, M. A. H.; Musa, O. M.; Armes, S. P. Combining Crystallization-Driven Self-Assembly with Reverse Sequence Polymerization-Induced Self-Assembly Enables the Efficient Synthesis of Hydrolytically Degradable Anisotropic Block Copolymer Nano-Objects Directly in Concentrated Aqueous Media. *J. Am. Chem. Soc.* **2024**, *146*, 16926–16934.
- (31) Skey, J.; O'Reilly, R. K. Facile One Pot Synthesis of a Range of Reversible Addition-Fragmentation Chain Transfer (RAFT) Agents. *Chem. Commun.* **2008**, 4183–4185.
- (32) Schindelin, J.; Arganda-Carreras, I.; Frise, E.; Kaynig, V.; Longair, M.; Pietzsch, T.; Preibisch, S.; Rueden, C.; Saalfeld, S.; Schmid, B.; Tinevez, J. Y.; White, D. J.; Hartenstein, V.; Eliceiri, K.; Tomancak, P.; Cardona, A. Fiji: An Open-Source Platform for Biological-Image Analysis. *Nat. Methods* **2012**, *9*, 676–682.
- (33) Nečas, D.; Klapetek, P. Gwyddion: An Open-Source Software for SPM Data Analysis. *Cent. Eur. J. Phys.* **2012**, *10*, 181–188.
- (34) Narayanan, T.; Sztucki, M.; Zinn, T.; Kieffer, J.; Homs-Puron, A.; Gorini, J.; Van Vaerenbergh, P.; Boesecke, P. Performance of the Time-Resolved Ultra-Small-Angle X-Ray Scattering Beamline with the Extremely Brilliant Source. *J. Appl. Crystallogr.* **2022**, *55*, 98–111.
- (35) Narayanan, T.; Sztucki, M.; Van Vaerenbergh, P.; Léonardon, J.; Gorini, J.; Claustre, L.; Sever, F.; Morse, J.; Boesecke, P. A Multipurpose Instrument for Time-Resolved Ultra-Small-Angle and Coherent X-Ray Scattering. *J. Appl. Crystallogr.* **2018**, *51*, 1511–1524.
- (36) Michael, S. SAXSutilities2: A Graphical User Interface for Processing and Analysis of Small-Angle X-Ray Scattering Data. Zenodo 2021.
- (37) Ma, B.; Wang, X.; He, Y.; Dong, Z.; Zhang, X.; Chen, X.; Liu, T. Effect of Poly(Lactic Acid) Crystallization on Its Mechanical and Heat Resistance Performances. *Polymer* **2021**, *212*, 123280.
- (38) Babichuk, I. S.; Lin, C.; Qiu, Y.; Zhu, H.; Ye, T. T.; Gao, Z.; Yang, J. Raman Mapping of Piezoelectric Poly(L-Lactic Acid) Films for Force Sensors. *RSC Adv.* **2022**, *12*, 27687–27697.
- (39) Chi, E.; Huang, H.; Zhang, F.; He, T. Nematic Phase of Plate-like Semicrystalline Block Copolymer Single Crystals in Solution Studied by Small-Angle X-Ray Scattering. *Langmuir* **2021**, *37*, 2397–2405.
- (40) Chi, E.; Huang, H.; Zhang, F.; He, T. Temperature-Enhanced Ordering in Plate-like Semicrystalline Block Copolymer Single-Crystal Suspensions Studied by Real-Time SAXS/WAXS. *Langmuir* **2025**, *41*, 5009–5020.
- (41) Roe, R.-J. *Methods of Neutron and X-Ray Scattering in Polymer Science*; Oxford University Press: New York, 2000.
- (42) Binks, B. P.; Lumsdon, S. O. Influence of Particle Wettability on the Type and Stability of

Surfactant-Free Emulsions. *Langmuir* **2000**, *16*, 8622–8631.

- (43) One reviewer has suggested that the true fractional surface coverage may be higher than that calculated owing to the presence of smaller platelet particles that cannot be resolved by confocal microscopy (see Figure 9). Bearing in mind the poor long-term stability observed for these platelet-stabilized Pickering emulsions, we do not necessarily agree with the reviewer. However, we cannot exclude their interpretation so it is acknowledged as a possibility.